Int J Adv Manuf Technol (2017) 93:2613–2623
DOI 10.1007/s00170-017-0541-5

ORIGINAL ARTICLE

Development of a modified through-mask electrochemical micromachining for micropatterning nonplanar surface

Pingmei Ming[1] · **Weihai Zhou**[1] · **Chenhao Zhao**[1] · **Hongmei Zhou**[1] · **Qin Ge**[1] · **Xinmin Zhang**[1]

Received: 2 January 2017 / Accepted: 7 May 2017 / Published online: 6 July 2017

Abstract To achieve cost-effective patterning of microfeatures on the nonplanar surfaces, a modified through-mask electrochemical micromachining process (TMEMM) was developed in which a layer of flexible insulating media with interconnected micropores is filled in the interelectrode gap and presses the through mask, considerably facilitating the mechanically attachment of the reusable through mask to the complex workpieces during EMM. A uniquely special tool cathode with a variety of outlet passages was correspondingly designed to significantly alleviate mass transfer limitation because of introduction of the flexible media. Some numerical and experimental investigations were then carried out to evaluate this proposed TMEMM process, with the focus on analyzing the dimension distribution uniformity of the machined microdimples. It is showed that the modified active TMEMM process exhibits favorable machinability and applicability to produce microdimples with significantly uniform geometric profiles on the planar and nonplanar surfaces.

Keywords Through-mask electrochemical micromachining · Flexible porous material · Surface texture · Reusable through mask · Electrochemical machining

✉ Pingmei Ming
mingpingmei@163.com

[1] Henan Polytechnic University, Jiaozuo 454000, People's Republic of China

1 Introduction

Electrochemical machining (ECM) is a nontraditional technique that removes workpiece materials by anodic dissolution process. It has been preferentially applied to remove difficult-to-machine metal materials and to manufacture complex features because of its some unique advantages over competing technologies. Through-mask electrochemical micromachining (TMEMM), in which workpiece is generally covered by an electrically insulating patterned photoresist, is one of the widely used electrochemical machining methods, mainly involving the production of microsized feature arrays such as microdimples and microholes [1–8]. In a standard TMEMM process, a nonconductive mask with a variety of perforated micropatterns is formed on the workpiece to define the features to be reproduced. The preparation of the through mask used in the traditional TMEMM processes generally involves a series of operations, including pretreatment of workpiece, spin coating of photoresist, prebaking, exposure, development, and postbaking, etc., and thus is tedious. Even so, such a through mask formed by photolithographic processes can be used only once and has to be remade repeatedly for each individual workpiece, which makes the TMEMM process costly and less suitable to the large-scale production. In addition, up to now, through mask is still extremely hard to be formed on the nonplanar surface (such as cylindrical surface) based on the photolithographic techniques. Therefore, the traditional TMEMM processes have some limitations in industrial applications.

To improve the traditional TMEMM processes, a variety of efforts have been made, especially focusing on facilitating mask making. Chauvy et al. [9–11] used the patterned oxide film as the through mask of TMEMM process, eliminating the need of photoresist masks, and realized the formation of microscaled features on the cylindrical workpiece.

Schönenberger et al. [12] applied the patterned photoresist mask to the cathodic tool instead of to the anodic workpiece, avoiding repetitious preparations of the patterned masks on the workpiece. Subsequently, Costa et al. [13, 14] further improved this kind of microfeature transferring process by using the patterned cathode with perforations through which the electrolyte can be pumped into the interelectrode gap. However, this transferring of through mask from the anode to the cathode may, to some degree, lead to the reduction in reproduction accuracy because of weaker confinement to the electrolytic current compared with the anode-base mask electrochemical micromachining (EMM). Zhu et al. [15–17] proposed an active through-mask electrochemical micromachining (active TMEMM) process in which the through mask is mechanically attached to rather than bonded to the workpiece, and can be reused repeatedly to other workpieces, avoiding repeated preparations of mask. Therefore, the active TMEMM process with the reusable mask is more efficient and more cost-effective compared to the standard TMEMM processes in mass production. Qu et al. [18–20] reported some modified TMEMM processes which use the removable patterned dry film as the cathodic tool or the anodic workpiece mask, and achieved a higher transfer accuracy of microfeature by periodically implementing anodic dissolution when the cathodic tool and the workpiece contact. The use of dry film simplifies preparation operations of the through mask by removing the need of mask making directly on the workpiece, and further facilitates the transfer of microfeatures to the nonplanar workpiece. Recently, to further improve the TMEMM process, Chen and Qu et al. [21–24] selected a polydimethylsiloxane (PDMS) material to make the reusable through mask mainly because it is more durable and has a better formability as a transferable mask compared to other EMM mask materials.

It can be seen from the recent studies that the use of reusable mask is a preferential alternative to prospectively make the TMEMM processes more applicable in the industrial practices. However, there is a vital issue needed to be first solved when the reusable and removable through mask is utilized. The issue is that how can the flexible through mask (like polypropylene sheet, dry film, and PDMS film) be fixed reliably and closely on the nonplanar solid surface? This is because that adhesive materials are not used to fix the reusable through mask and a well-determined gap between the cathode and the through mask is required to allow the electrolyte to flow in and out during anodic dissolution. Some investigators [23–25] have made their efforts to mechanically fix the removable mask on the workpiece by using fixing block or fixing micropillars, but these measurements were founded to be less controllable and less effective, because the fixtures used are very difficult to make the mask be fully and closely attached to the nonplanar surfaces and also unavoidably affect the electrolyte motion within the interelectrode gap during machining.

In this paper, a modified TMEMM process with reusable mask is proposed with the expectation of greatly improving the applicability of the active TMEMM by optimizing the fixing and position way of the through mask on the curved surfaces. In the modified active TMEMM, the removable flexible insulating through mask is attached mechanically to the workpiece via a layer of flexible nonconductive porous material which is right in contact with the through mask and is pressed by a cathode assembly. The introduced porous material filled within the interelectrode gap is about 0.5–2 mm thick and can offer passages for the electrolyte during machining. Therefore, the proposed active TMEMM is called a gap-filled active TMEMM here because the gap between the through mask and the cathode in the traditional TMEMM processes is only filled solution and some by-products. In the following sections, we will investigate numerically and experimentally the gap-filled active TMEMM process, including analyzing distribution characteristics of the flow field and initial current field within the interelectrode gap and evaluating the dimension distribution of the microdimples created on the planar and nonplanar workpieces.

1.1 Design of the cathode assembly for the gap-filled TMEMM

Since the porous material is introduced into the interelectrode gap of TMEMM, it is inferred that the mass transfer within the interelectrode gap during machining is probably weakened. Therefore, in this research, the cathode was specially designed by introducing some nontraditional structures to relieve the possible mass transportation limitation. The design concept of the cathode is to allow the electrolyte to flow in and out the interelectrode gap through multiple flow passages arranged in the entire cathode, as illustrated schematically in Fig. 1. Figure 2 shows the detailed designs of the cathode and its assembly with the anode used for TMEMM of the planar surface. The pliant porous nonconductive media is filled between the cathode and the mask which attaches closely to the workpiece (the anode). Unlike the conventional cathode, the cathode used here contains various flow passages, including general inlet, collecting well, flow-in channel, flow-out channel, electrolyte sub-inlet, and electrolyte outlet, etc. The flow-in channel in which some electrolyte sub-inlets are arranged and the flow-out channel in which some electrolyte outlets are arranged are set alternately in the entire cathode to allow the solution to flow in and out the interelectrode gap all aroundly. To avoid interfering between in-flowing and out-flowing motions of electrolyte, a sealing pad and a cover plate are additionally designed. To enable the mask to be attached very closely to the workpiece, a proper pressure applied to the cover plate is needed. With these uniformly distributed flow

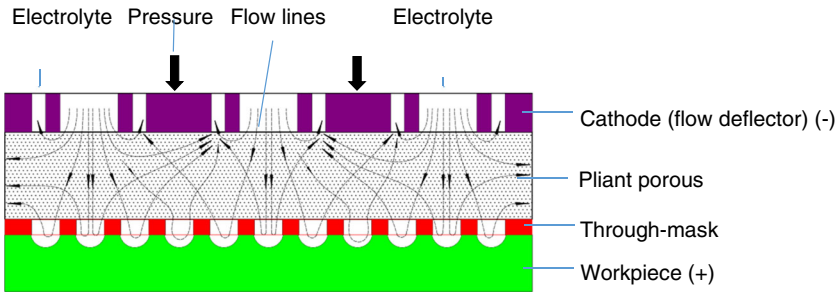

Fig. 1 Schematic diagram of the gap-filled TMEMM

passages, the mass transfer conditions are expected to be very good and are hardly dependent on the workpiece size during machining.

During working, the electrolyte is pumped into the collecting well through the general inlet and then is pressed into the porous media through both the flow-in channels and the electrolyte sub-inlets; after that, a fraction of the electrolyte in the porous media goes into the cavities formed by the through mask and the workpiece surface to serve the electrochemical reactions and then flows out the cavities with some electrolytic products. The discharge of the electrolyte from the cavities is likely to have two ways: besides a very small fraction of it flows out through the peripheral micro-pores of the porous media, the majority gets out through the discharging features arranged in metallic flow deflector, schematically shown in Fig. 1. When the machining is finished, the cathode assembly, the porous media, and the through mask can be reused repeatedly in another similar machining

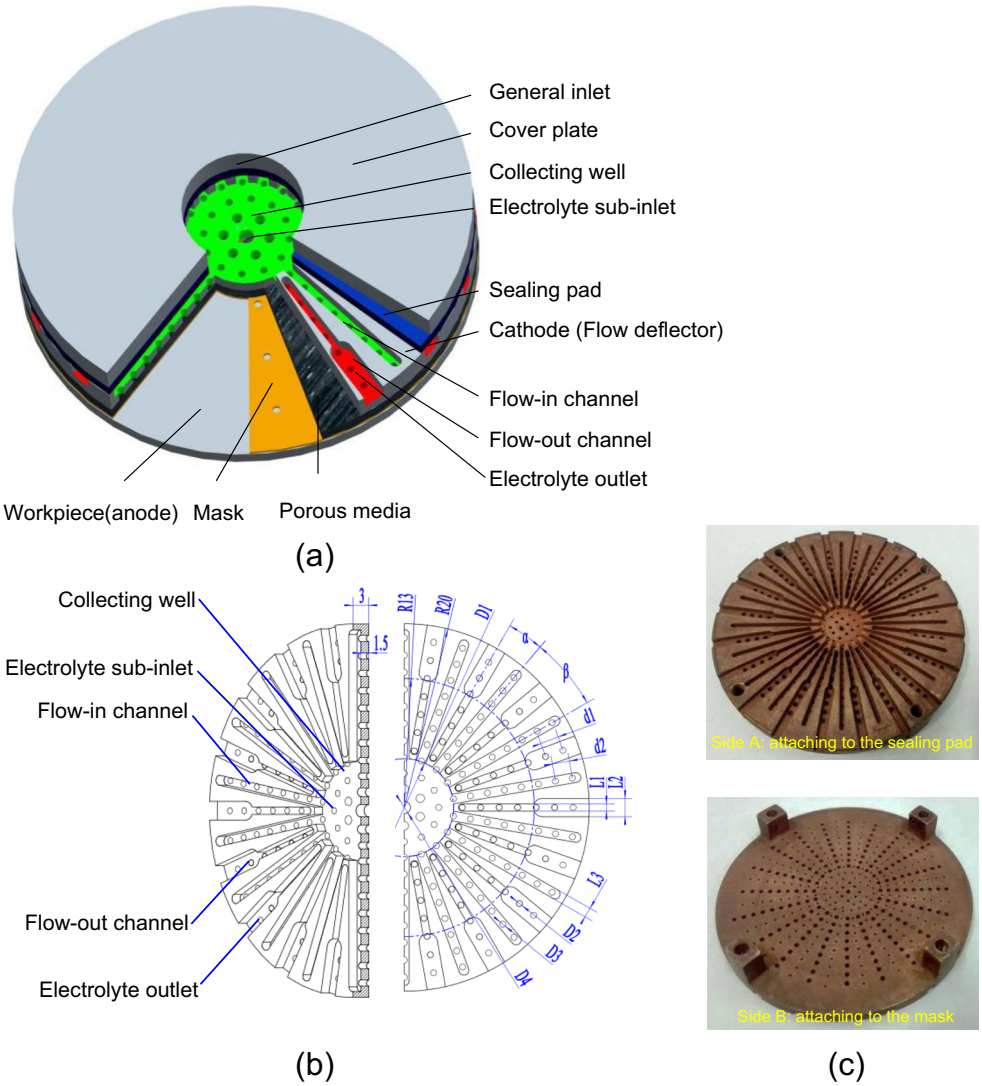

Fig. 2 The designed cathode and its assembly with the anode. **a** Cathode-anode assembly. **b** Flow deflector geometry and its main dimensions. **c** Photos of the cathode

practices. Therefore, for the proposed TMEMM process, on the one hand, more desirable attachment of the mask both to the planar surface and to the curved surface (if shaped cathode is employed) can be obtained because of the flexibility and pliancy of the porous media used; on the other hand, favorably better mass transfer conditions with a significantly homogenous flow field and a relatively prompt discharging of the by-products can be achieved due to the introduction of the special cathode assembly.

1.2 Analysis of the interelectrode flow field

Unlike the traditional TMEMM processes in which the interelectrode gap is normally filled with only the electrolyte and some by-products, the proposed TMEMM process has an additional porous media within its gap which is also filled by the electrolyte and the by-products. The existence of the nonconductive porous media may inevitably influence the interelectrode flow field properties, although the cathode assembly was subtly designed and used. Since the porous media are assumed to be homogeneous in the material properties and the thickness, it thus is considered to have uniformly distributed Ohm's resistance to the anodic dissolution processes in this paper. In the following, numerical analysis of the flow field is carried out.

Two physical models were established for the simulation of the interelectrode flow field, which represented two modes for electrolyte discharging: inside mode—discharging mostly from the outlet passages (with multiple outlet passages inside the cathode), and outside mode—discharging completely from the from the interelectrode gap peripheral opening because no outlet passages are set inside the cathode, as shown in Fig. 3.

To facilitate simulation, some assumptions are made. (1) the properties (including porosity and pore sizes) and the thickness of the pliant porous media are homogeneous; (2) the electrolyte temperature keeps constant and is the same everywhere; (3) the electrolyte is a solution of single-phase and does not contain solid- and gas-phase substance; (4) the time considered for the simulations is very short, neglecting the influence of anodic dissolution process on the flow field; (5) no electrolyte exists at the interfaces between porous media and mask, and mask and workpiece; (6) pressure of electrolyte outlet is set to be 1 atm. The simulations were carried out using the software FLUENT 6.3, and the parameters used for numerical analysis are listed in Table 1. Since our previous researches have shown that the geometry parameters of the cathode assembly including D1, D4, d2, and d1 (see Fig. 2b) are vital to the flow field distribution within the interelectrode gap, they are specially optimized by numerical analysis here and the calculation procedures are shown in Fig. 4.

Figure 5a shows the flow field distribution on the whole workpiece based on the optimized parameters of D1 = 10 mm, D4 = 0.8 mm, d2 = 2 mm, and d1 = 3 mm. Generally, uniform flow field with the same order of flow velocities ranging from 1×10^{-2} to 2×10^{-2} m/s can be obtained over the whole porous media except the regions where the sub-inlets and outlets of the cathode-deflector unit are responded to. In the

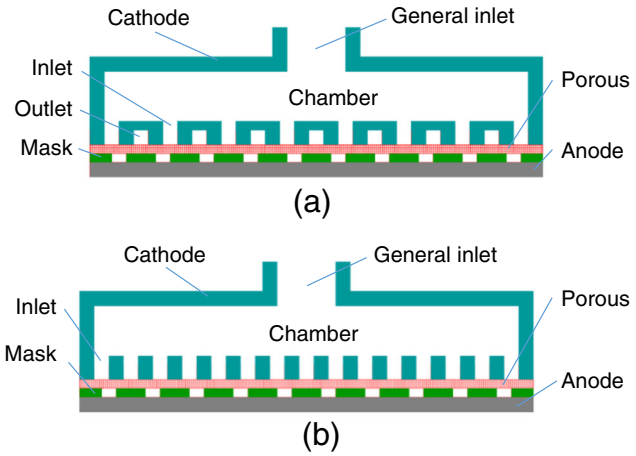

Fig. 3 Physical model for the simulation of the flow field during gap-filled TMEMM with two different discharging modes. **a** With multiple outlet passages. **b** Without multiple outlet passages

Table 1 Main parameters and values used for the analysis of the flow field

Items	Values or variables
Electrolyte	20 wt% $NaNO_3$
Temperature/T	25 °C
Input pressure of electrolyte/P	1 MPa
Flexible porous material (polypropylene) thickness/h	0.2 mm
Porosity of flexible porous material	70~75%
Pore size of flexible porous material	0.8–1.2 μm
Diameter of collecting well/D1	10 mm
Cathode diameter	40 mm
Diameter of electrolyte outlet/D2	0.5 mm
Diameter of electrolyte sub-inlet/D3	0.5 mm
Diameter of electrolyte sub-inlet in the collecting well/D4	0.8 mm
Diameter of workpiece anode	40 mm
Flow-out channel width/L1	1 mm
Flow-out channel width/L2	2 mm
Flow-in channel width/L3	1 mm
Angle between two neighboring inlet channel/β	22.5°
Angle between inlet and outlet channel/α	11.25°
Distance between two neighboring outlets of electrolyte/d1	3 mm
Distance between two neighboring inlets of electrolyte/d2	2 mm
Force on flexible porous material	5 N
Cathode thickness	3 mm
Channel depth	1.5 mm

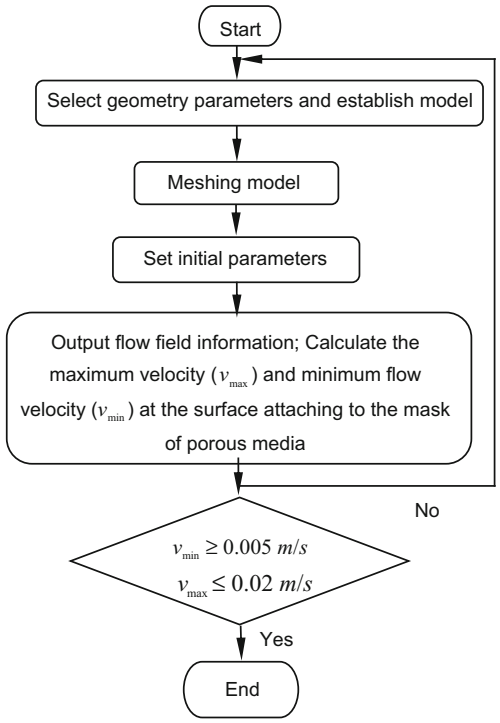

Fig. 4 Flow diagram of optimizing geometry parameters of the cathode assembly by simulating the interelectrode flow field

abovementioned regions, the flow rates are slightly smaller. Furthermore, the electrolyte flow within individual cavity has a closely identical flow pattern and approximately the same flow rate (see Fig. 5c). For comparative analyses, the flow field in the filled interelectrode gap using the conventional cathode structure with only electrolyte inlets was computed. It was found that if the additional outlet passages were not arranged inside the cathode, the flow rates are much lower (about 6×10^{-4}–4×10^{-3} m/s) and also vary significantly even though the cathode was optimally designed, as shown in Fig. 5b.The findings from the above simulations indicated that fairly desirable electrolyte flow conditions can be achieved for the anodic dissolution processes if the special cathode structure was applied to the gap-filled TMEMM processes.

2 Experimental

The process conditions and parameters utilized here are the same as the simulation operations shown in Table 1. A stainless steel (SUS304) plate with a diameter 40 mm was served as the workpiece. To facilitate providing of fresh electrolyte and removal of dissolved products, pulsed currents (pulse duration 10 ms) were applied to the machining processes with the voltages ranging from 12 to 16 V and the pulse duty ratios of 1:2, 1:3, or 1:4. The external force acting on the cathode-deflector was 5 or 7 N. The thickness of the through mask is selected to be 0.1 and 0.2 mm, and the diameter of the mask perforations which are made by CNC drilling is 0.5 mm, that is, the aspect ratio of the polyvinyl chloride (PVC) through mask perforations is 0.2 or 0.4, respectively. The total machining time was 3 min. A digital microscope (KEYENCE VHX-2000, Japan) was employed to characterize the shape profile of the machined microdimples, and a scanning electron microscope (Hirox Mini-SEM SH-4000, Japan) was adopted to observe the morphologies and topographies of the produced microdimples. The surface roughness of the machined microdimples was evaluated by using a white light interferometer (Talysurf CCI6000, UK). To analyze the uniformity of geometric dimensions of the machined microdimples over the entire workpiece, 13 perforations were selectively arranged in the through mask to correspondingly obtain 13 etched microdimple at the representative regions of the workpiece, as illustrated in Fig. 6. The geometric dimensions of the machined 13 microdimples on each sample were then measured, and the microdimple's diameter and depth were obtained.

3 Results and discussion

3.1 Profile characteristics of machined microdimples

As shown in Fig. 7, all 13 microdimples machined under the optimized conditions show a closely identical cone-shaped profile which is very less relevant to the position of the microdimple at the workpiece and thus possess an excellent geometric profile consistency. The machined surface of the microdimples is significantly smooth, the surface roughness Ra being 1.35–3.56 μm. It can be concluded that the proposed gap-filled TMEMM process has the potentiality of achieving highly identical microsized features.

3.2 Effect of applied voltage on microdimple's geometric dimensions

Our previous initial experiments demonstrated that if the applied voltages were smaller than 10 V, the dissolution rate during machining was extremely slow. Therefore, the voltages selected for the current experiments were all greater than 10 V. Figure 8 shows the relationships between the applied voltage and the geometric dimensions (diameter and depth) of the 13 microdimples produced. It can be seen in Fig. 8 that the geometric dimensions of the machined microdimple have a certain dependence on the applied voltage. Although the average value of the geometric dimensions (average diameter, average depth) of all the 13 formed features increases very slightly with increasing the applied voltage, changing within a narrow range of 618–628 μm in diameter and 18–27 μm in depth, the dimension distribution characteristics of the microdimples alter significantly. The dimension distribution uniformity of the machined microdimples becomes increasingly better with decreasing the

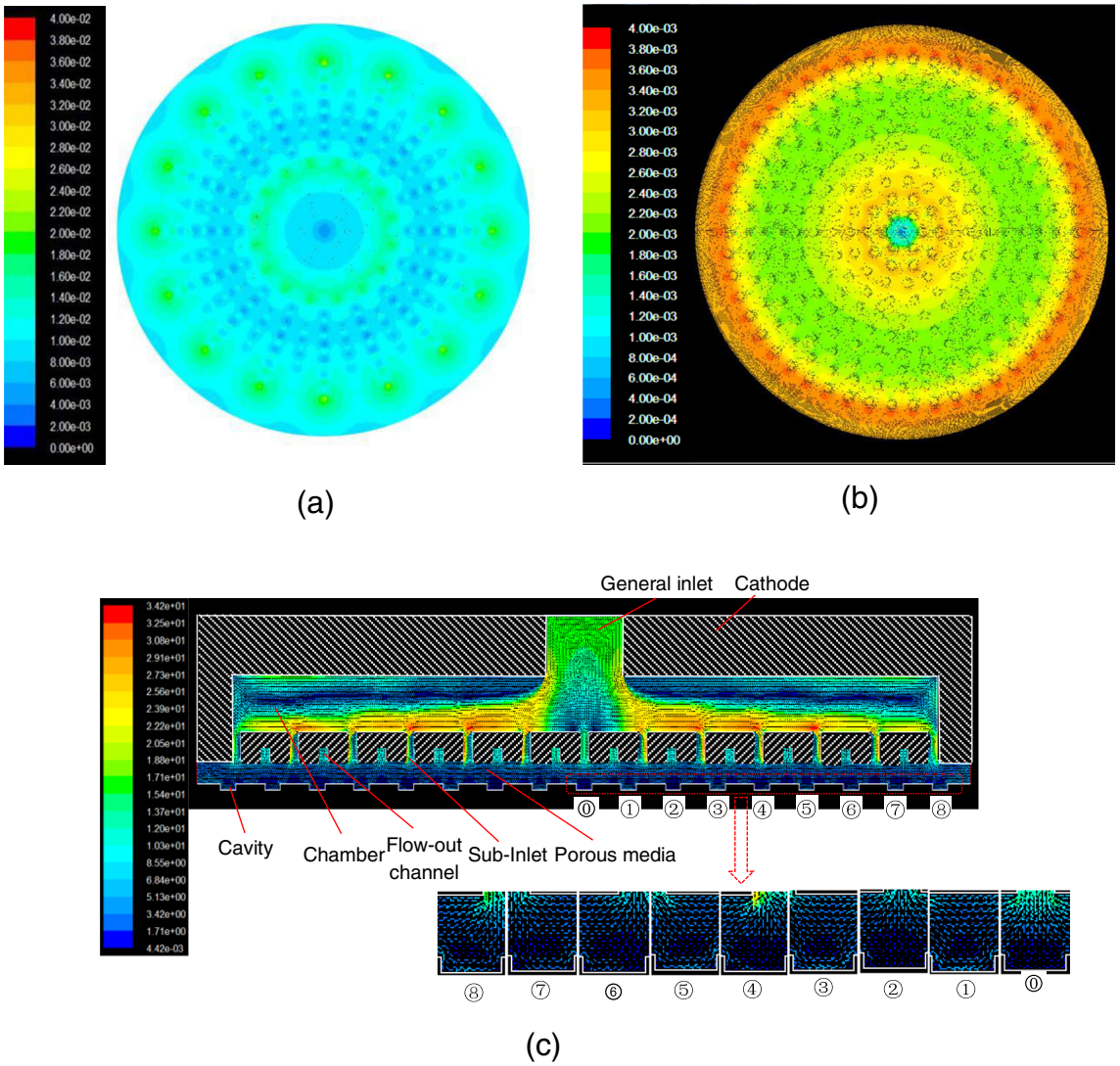

Fig. 5 Flow field distribution within the interelectrode gap of the gap-filled TMEMM when the optimized cathode is used. **a** Flow field distribution at the surface attaching to the mask of the porous media when multiple outlet. **b** Flow field distribution at the surface attaching to the mask of the porous media when no multiple. **c** Flow field distribution within the mask cavity when using multiple outlet passages

applied voltage, while, at the same time, smaller and shallower microdimples are obtained. For example, the standard deviations (STDEV) of the diameter and the depth of the 13 microdimples are only 7.27 and 3.73 μm, respectively, at 12 V (see Fig. 8b), while they rise to 15.19 and 25.54 μm at 14 V (see Fig. 8c), and

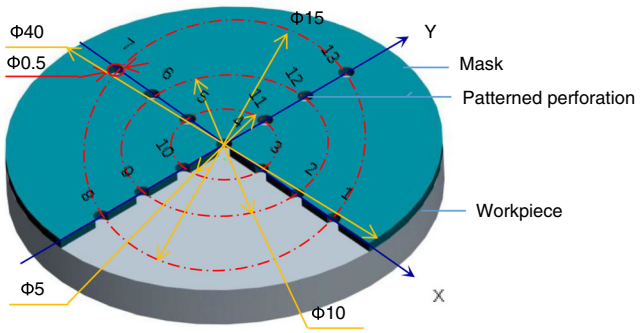

Fig. 6 Position of the microdimples to be formed on the workpiece

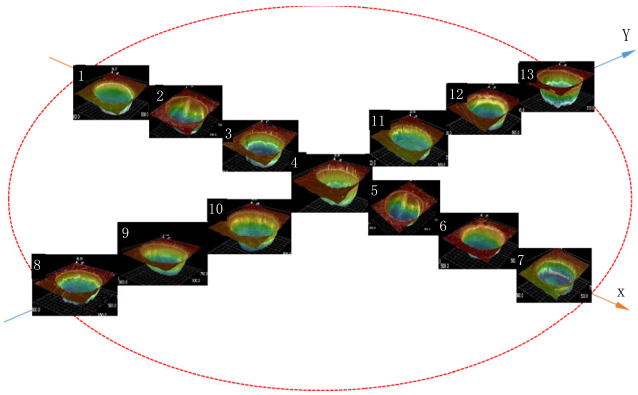

Fig. 7 Three-dimensional profile of the 13 microdimples machined with optimal process parameters

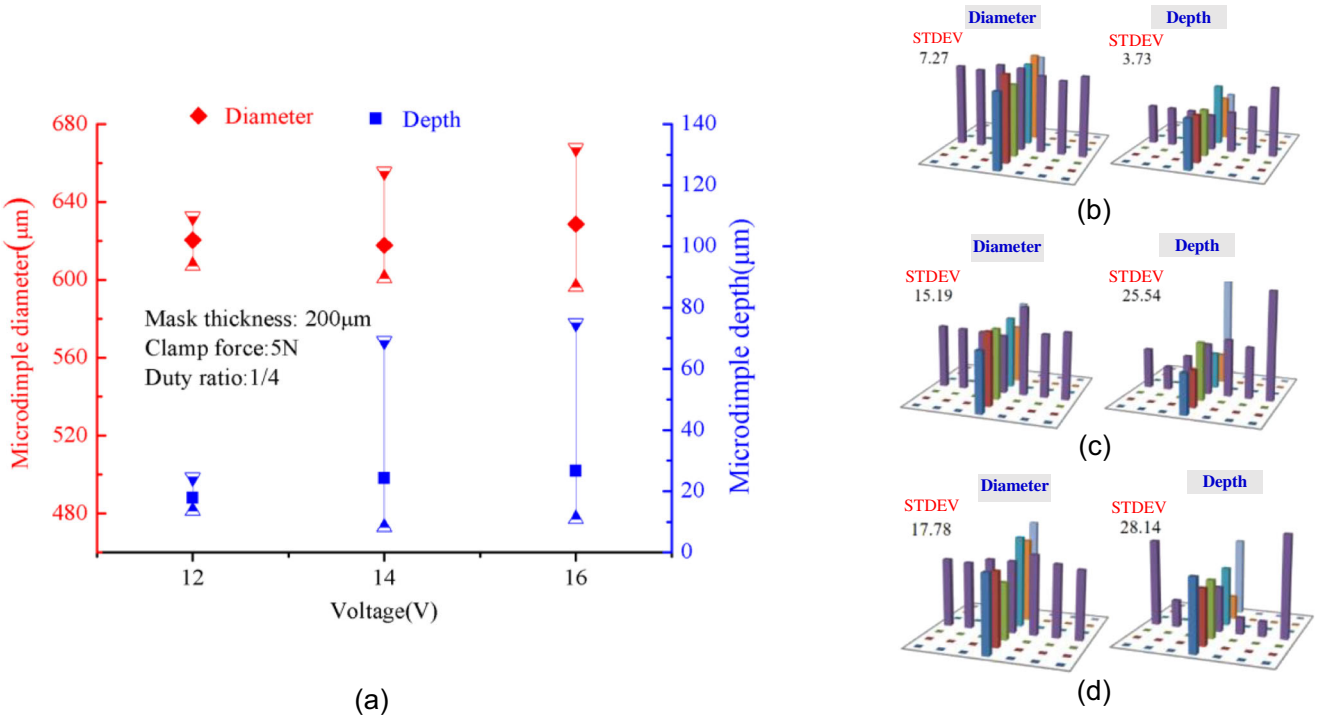

Fig. 8 Variation of the geometric dimensions' distribution of 13 machined microdimples with the applied voltage. **a** Variation of geometric dimension with the applied voltage. **b** The geometric dimension's distribution at 12 V. **c** The geometric dimension's distribution at 14 V. **d** The geometric dimension's distribution at 16 V

up to 17.78 and 28.14 μm at 16 V (see Fig. 8d). The reasons for these variations could be that the filled porous media between the mask and the cathode prevent, to some degree, the electrolyte from flowing sufficiently fast to serve the higher applied voltage situations, where more fresh electrolyte and faster mass transfer rate are required to accommodate the electrochemical reactions and the removal of the electrolytic products. Thus, to obtain the microdimples with reduced geometric dimension deviations, relatively small voltages are suggested. In the following experiments, 12 V voltage was selected.

3.3 Effect of external force on microdimple's geometric dimensions

Since the compression deformation degree of the flexible porous polypropylene film used for this research is sensitive to the external pressure that the porous media is received, the seepage performance of the porous media unavoidably changes with the applied pressures. In our experiments, the external force pressing on the media was selected to be 5 and 7 N, representing a light pressure and a heavy pressure used, respectively. Figure 9 shows the effect of external force acting on the porous media on the machined microdimple's geometric dimensions. The data from Fig. 9 really confirmed that the microdimple's profile feature and its geometric dimension distribution are very subtle on the external force applied to the media. When the force is 5 N, the diameter and depth of the microdimple are 607–632 μm (average value 620 μm, STDEV 7.27 μm) and 14–26 μm (average value 18 μm, STDEV 3.73 μm) (shown in Fig. 9a, b), the microdimples appear highly similar in the shape. While, when the force is 7 N, the geometric dimensions of the machined microdimples show a big difference, changing in the range of 571–642 μm (average value 606 μm) in diameter and 16–95 μm (average value 43 μm) in depth and their STDEV is up to 22.86 and 25.57 μm, respectively, as shown in Fig. 9a, c. This is because that the porous media become more compressed when the external force is bigger, which leads to a more serious hindering effect on the mass transfer during the anodic dissolution, and a significantly limited mass transfer condition further deteriorates the electric field distribution. Consequently, appropriately small pressure on the porous media should be selected during the machining. As an optimized value in this research, 5 N was determined.

3.4 Effect of pulsed current duty ratio on microdimple's geometric dimensions

Figure 10 shows the effect of the applied pulsed current duty ratio on the machined microdimple's profile. With a constant

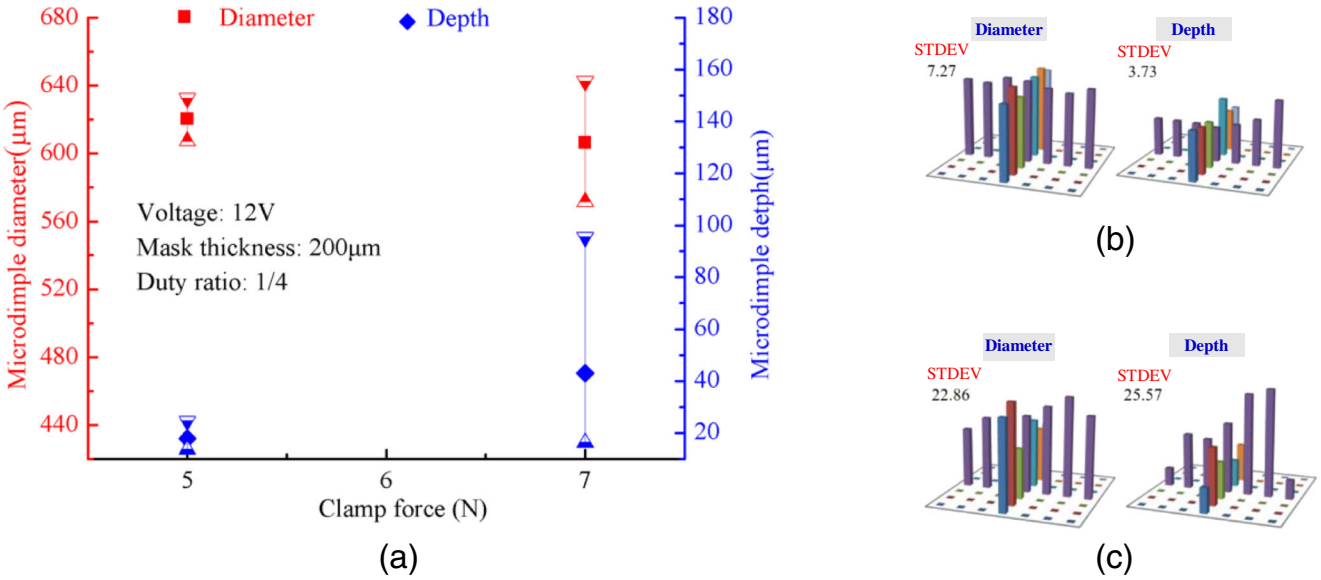

Fig. 9 Variation of the geometric dimensions' distribution of 13 machined microdimples with the applied external force. **a** Variation of geometric dimension with the applied external force. **b** Ggeometric dimension's distribution at 5 N. **c** Geometric dimension's distribution at 7 N

pulse duration, the dimension distribution of the machined microdimples improves with decreasing the duty ratio. When the duty ratio is 1:2, the diameter and depth of the machined microdimples range in 610–657.2 μm (average 637.5 μm) and 25.6–57.7 μm (41.2 μm) and both of them show a dispersive distribution, the STDEV being 15.39 μm in diameter and 12.39 μm in depth (see Fig. 10d), while, as the duty ratio is reduced, the dimension differences of the machined microdimples correspondingly drop. For example, when the smallest duty ratio, 1:4, is chosen, the dimension deviation of the microdimples over the entire workpiece is correspondingly smallest (see Fig. 10b), and thus, the profile of the machined microdimples shows the best uniform distribution but at the cost of shallowing the microdimples. Therefore, from the viewpoint of achieving uniform microfeatures, an appropriately small duty ratio of the pulsed

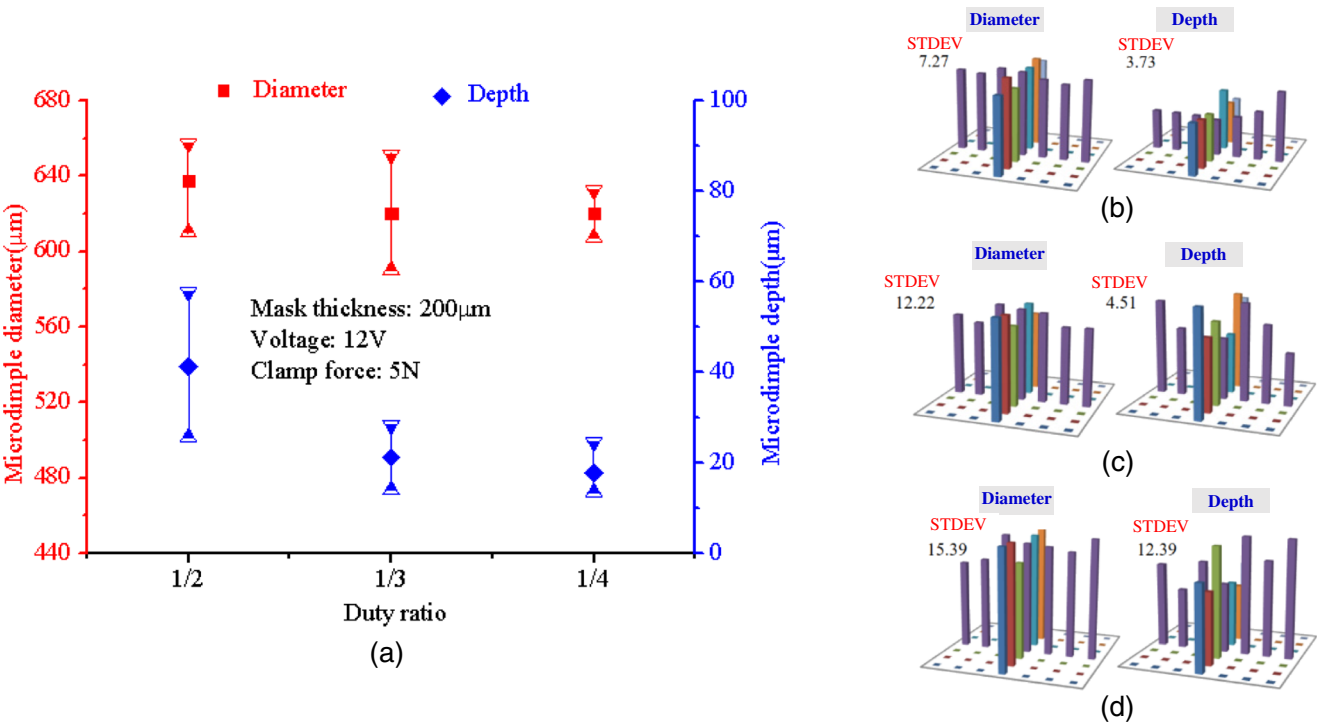

Fig. 10 Variation of the geometric dimensions' distribution of current. **a** Variation of geometric dimension with the applied external duty ratio. **b** Ggeometric dimension's distribution at 1/4. **c** Geometric dimension's distribution at 1/3. **d** Geometric dimension's distribution at 1/2

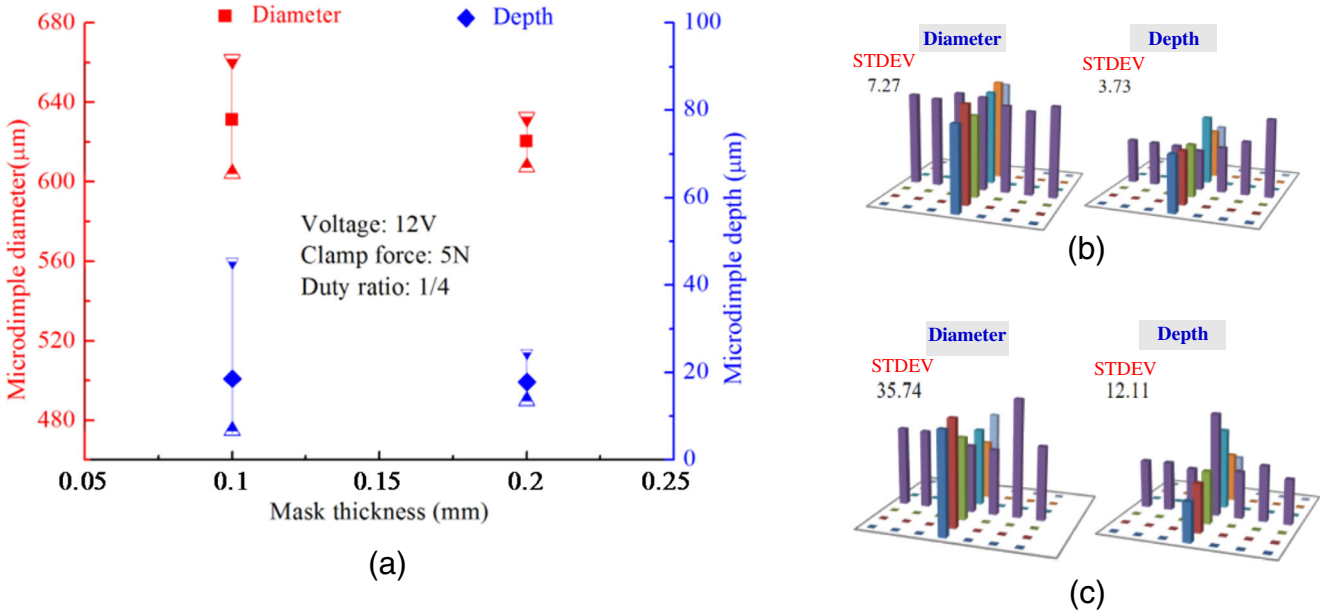

Fig. 11 Variation of the geometric dimensions' distribution of 13 machined microdimples with the applied mask thickness. **a** Variation of geometric dimension with the applied mask thickness. **b** Ggeometric dimension's distribution at 0.2mm. **c** Geometric dimension's distribution at 0.1mm

current is recommended to leave more interval time for the electrolytic products to discharge away.

3.5 Effect of mask thickness on microdimple's geometric dimensions

Researches [6–10] have revealed that the mask thickness and aspect ratio of the perforations of the mask give some substantial effects on the profile characteristics of the machined microfeatures including overcut during through-mask electrochemical machining. For this modified TMEMM, a similar conclusion was found in Fig. 11 which illustrates the influence of mask thickness on the microdimple's dimensions. For instance, as shown in Fig. 11b, when the mask thickness is 0.2 mm, the dimensional deviations of the microdimples are very small, while, when the mask thickness is 0.1 mm, the dimension deviations get remarkably bigger with the diameter's standard deviation being 35.74 μm and the depth's standard deviation being 12.11 μm (see Fig. 11c). On the other

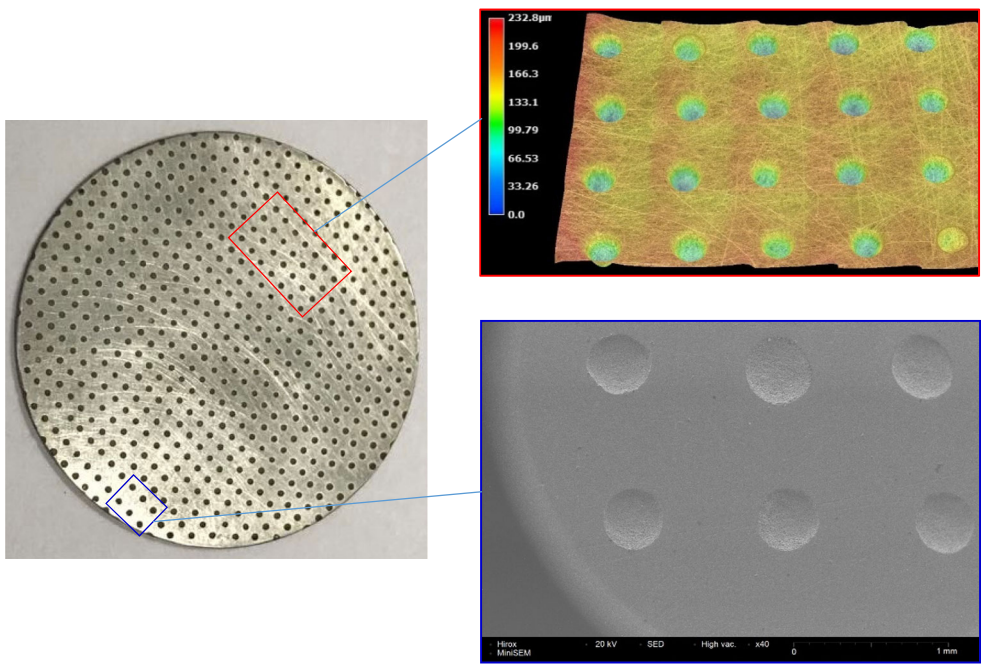

Fig. 12 Morphologies of the microdimples machine on the planar workpiece

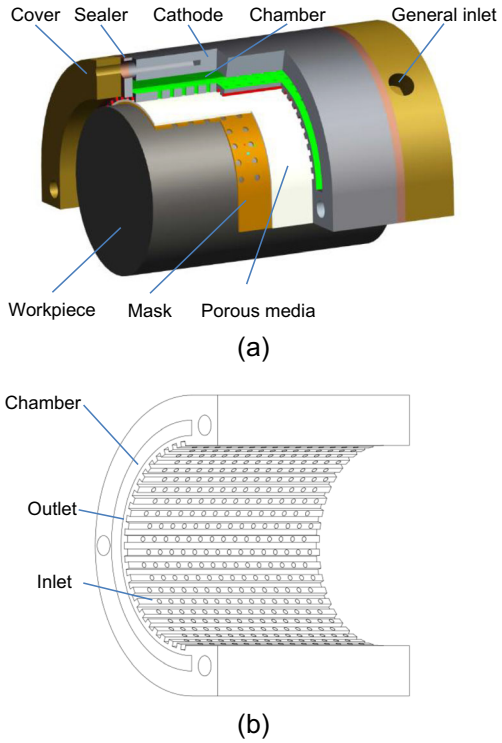

Fig. 13 Cathode assembly designed for the formation of microdimple arrays on the cylindrical surface. **a** Cathode-anode assembly. **b** Cathode

hand, few islands can be observed within the microdimple when the mask thickness is 0.2 mm, in contrast, islands are formed sometimes if the 0.1-mm-thick mask is utilized. The involved reasons for the above differences have been disclosed in the literatures [6–10]. As a rule, for the TMEMM process, a properly thick mask can be beneficial to form uniform microdimples.

3.6 Machining of microdimple arrays on planar and cylindrical surface

To further evaluate feasibility of the presented gap-filled TMEMM process, the microdimple arrays were formed on the planar workpiece (SUS304 stainless steel, diameter 40 mm) and on the cylindrical workpiece (SUS304 stainless steel, diameter 48 mm). The perforation diameter of the mask used is 500 μm for the planar surface and the cylindrical surface. As shown in Fig. 12, the geometric profile of the microdimples machined on the planar surface shows a good similarity, with its diameter changing in the range of 351.3–377.4 μm and its depth in the range of 15.3–18.1 μm; besides, the surface of the microdimples machined is fairly smooth.

The formation of microdimple arrays on the cylindrical surface was achieved by using a specially designed cathode assembly which adopts the same design concept used for the planar surface, as shown in Fig. 13. The whole cylindrical surface was machined by three times, 120° central angel per time. Figure 14 shows the microdimples machined on the cylindrical surface. It is shown from the data obtained by measuring 30 microdimples selected randomly that the geometric dimension distribution of the microdimples shaped is acceptably uniform with the diameter being 605.3–624.9 μm and the depth being 11.5–18.9 μm. These findings indicated that generally homogenous microdimples can be achieved both on the planar surface and on the cylindrical surface.

4 Conclusions

To further extend the process ability and the applicability of TMEMM processes, a modified through-mask electrochemical micromachining process was proposed, named gap-filled TMEMM, in which a flexible insulating media with interconnected micropores are filled between the reusable through mask and the cathode. To favorably functionalize the newly proposed TMEMM, a special cathode with multiple outlet passages was designed which can allow the electrolyte and the electrolytic products to discharge away efficiently and swiftly. Some simulations and experiments were carried out to evaluate this process. The conclusions made from this research are as follows:

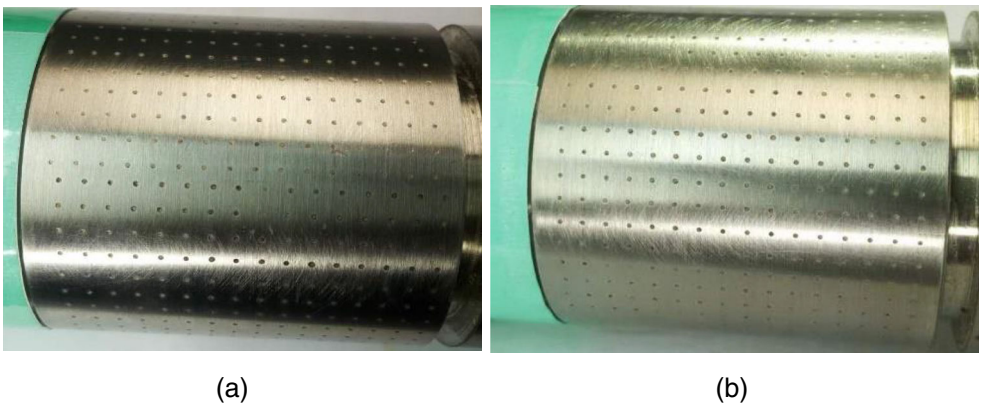

Fig. 14 Microdimple arrays machined on the cylindrical surface. **a** Zero–180° half-cylindrical surface. **b** One hundred eighty–360° half-cylindrical surface

1. A good attachment of the flexible thin through mask to both the planar surface and cylindrical surface to be patterned can be achieved with the pressures of pliant porous media.
2. Multiple outlet passages should be arranged within the cathode to relieve mass transfer limitation caused by the filled porous media during the machining.
3. The geometric dimensions and their distribution characteristics of the microdimples machined were dependent on applied voltage, external pressure applied to the flexible porous media, mask thickness, and duty ratio of pulsed current.
4. The microdimples with a high similarity in three-dimensional profiles and a relatively smooth surface can be patterned both on the planar surface and on the cylindrical surface using the gap-filled TMEMM process.

Acknowledgements This work was financially supported by the National Natural Science Foundation of China (no. 51475149), the Program for Science and Technology Innovation Team in Universities of Henan Province (no. 15IRTSTHN013); and the Program for Science and Technology Innovation Team in Henan Polytechnic University (no. T2014-1).

References

1. West AC, Madore C, Matlosz M, Landolt D (1992) Shape changes during through-mask electrochemical micromachining of thin metal films. J Electrochem Soc 139(2):499–506
2. Shenoy RV, Datta M, Romankiw LT (1996) Investigation of island formation during. through-mask electrochemical micromachining. J Electrochem Soc 143(7):2305–2309
3. Datta M (1998) Microfabrication by electrochemical metal removal. IBM J Res Dev 42(5):655–670
4. Datta M, Landolt D (2000) Fundamental aspects and applications of electrochemical microfabrication. Electrochim Acta 45(15): 2535–2558
5. McCrabb H, Lozano-Morales A, Snyder S (2009) Through mask electrochemical machining. ECS Trans 19(26):19–33
6. Zhu D, Qu NS, Li HS et al Electrochemical micromachining of microstructures of micro hole and dimple array. CIRP Ann Manuf Technol 58(1):177–180
7. Qian SQ, Zhu D, Qu NS (2010) Generating micro-dimples array on the hard chrome-coated surface by modified through mask electrochemical micromachining. Inter J Adv Manuf Technol 47(9–12): 1121–1127
8. Chen XL, Qu NS, Li HS, Xue ZX (2015) Pulsed electrochemical micromachining for generating micro-dimple arrays on a cylindrical surface with a flexible mask. Appl Surf Sci 343:141–147
9. Chauvy PF, Madore C, Landolt D (1999) Electrochemical micromachining of titanium through a patterned oxide film. Electrochem Solid-state Lett 2(3):123–125
10. Chauvy PF, Hoffmann P, Landolt D (2001) Electrochemical micromachining of titanium through a laser patterned oxide film. Electrochem Solid-State Lett 4(5):C31–C34
11. Chauvy PF, Hoffmann P, Landolt D (2003) Applications of laser lithography on oxide film to titanium micromachining. ApplSurf Sci 208:165–170
12. Schönenberger I, Roy S (2005) Microscale pattern transfer without photolithography of substrates. Electrochim Acta 51(5):809–819
13. Costa HL, Hutchings IM (2009) Development of a maskless electrochemical texturing method. J Mater Process Technol 209:3869–3878
14. Parreira JG, Gallo CA, Costa HL (2012) New advances on maskless electrochemical texturing (MECT) for tribological purposes. Surf Coat Technol 212:1–13
15. Zhu D, Qu NS, Li HS (2009) Electrochemical micromachining of microstructures of micro hole and dimple array. CIRP Ann Manuf Technol 58:177–180
16. Li DL, Zhu D, Li HS (2011) Effects of mask wall angle on matrix-hole shape changes during electrochemical machining by mask. J Cent South Uni Tech 18:1115–1120
17. Li DL, Zhu D, Li HS (2011) Microstructure of electrochemical micromachining using inert metal mask. Int J Adv Manuf Technol 55:189–194
18. Qu NS, Chen XL, Li HS, Zeng YB (2014) Electrochemical micromachining of micro-dimple arrays on cylindrical inner surfaces using a dry-film photoresist. Chin J Aeronaut 27:612–618
19. Zhang X, Qu NS, Li HS (2015) Investigation of machining accuracy of micro-dimples fabricated by modified microscale pattern transfer without photolithography of substrates. Int J Adv Manuf Techno 81(9–12):1475–1485
20. Qu NS, Zhang XF, Chen XL (2015) Modified microscale pattern transfer without photolithography of substrates. J Mater Process Technol 218:71–79
21. Chen XL, Qu NS, Li HS (2014) The fabrication and application of a PDMS micro through-holes mask in electrochemical micromanufacturing. Adv Mech Eng 6:1–7
22. Chen XL, Qu NS, Li HS (2015) Removal of islands from micro-dimple arrays prepared by through-mask electrochemical micromachining. Precis Eng 39:204–211
23. Chen XL, Qu NS, Li HS (2016) Electrochemical micromachining of micro-dimple arrays using a polydimethylsiloxane (PDMS) mask. J Mat Process Technol 229:102–110
24. Chen XL, Qu NS, Li HS (2015) Pulsed electrochemical micromachining for generating micro-dimple arrays on a cylindrical surface with a flexible mask. Appl Surf Sci 343:141–147
25. Li DL. Application and fundamental research of multiple holes by electrochemical machining using mask. Nanjing: Nanjing University of Aeronautics and Astronautics (in Chinese)